Driver Assistance Controller for Tire Saturation Avoidance up to the Limits of Handling

Conference Paper · October 2015

DOI: 10.1109/LARS-SBR.2015.73

2 authors:

Carlos M. Massera
University of São Paulo
18 PUBLICATIONS **45** CITATIONS
SEE PROFILE

Denis Wolf
University of São Paulo
138 PUBLICATIONS **1,363** CITATIONS
SEE PROFILE

Driver Assistance Controller for Tire Saturation Avoidance Up to the Limits of Handling

Carlos Massera Filho[1], Denis F. Wolf[1]

***Abstract*— Electronic Stability Control (ESC) reduced the number of fatal crashes in single vehicle accidents in 32%, a ESC unit corrects the vehicle yaw rate avoiding under-steering or over-steering in relation to the drives intent. In recent years Steer-by-Wire systems have been proposed for driver assistance systems, this allows the development of controllers capable of predicting and avoiding exceeding saturation limits. This paper proposes a Model Predictive Controller to safely handle longitudinal and lateral driver intents up to the limits of handling on front wheel driven vehicles.**

I. INTRODUCTION

In past years several technologies have been introduced to mass produced vehicles in order to reduce the number of injuries and fatalities during crashes. One example of such technologies is Electronic Stability Control (ESC) which reduced the number of fatal crashes in single vehicle accidents in 32% [1]. A ESC unit corrects the vehicle yaw rate avoiding under-steering or over-steering in relation to the drives intent.

Recently, Steer-by-Wire systems have been proposed for driver assistance systems. These consists in eliminating the mechanical coupling between the drivers steering wheel and the front wheel. In 2010, Hsu et al. [2] demonstrated that a Steer-by-Wire system allowed friction estimation based on the steering torque and Hamann et al. [3] proposed a faster converging method based on Unscented Kalman Filter. The capability of directly control each steerable wheel aligned with the ability to measure saturation limits allows the development of controllers capable of predicting and avoiding exceeding saturation limits.

Control community have been increasingly adopting Model Predictive Control (MPC) for its ability to correct not only a current state error but also a future predicted error while modeling state and input constraints in a intuitive form. Beal and Gerdes [4] applied MPC technique combined with envelope control to smoothly enforce control boundaries in coordination with a human driver. They proposed a linear bicycle model variation named Affine Force Input (AFI) that represented the tire nonlinearities during a show horizon while allowing a convex optimization. Carvalho et al. [5] proposed a MPC for evasive maneuvers based on the iterative linearization of a nonlinear Ackerman model with convexified constraints. In most assistive shared steering controllers, the longitudinal and lateral driver intents are modeled separately and two controller are developed for those problems.

* This work was supported by CNpQ and FAPESP

[1]Institute of Mathmatics and Computer Science, University of São Paulo, Avenida Trabalhador São-carlense, 400, São Carlos, Brazil massera,denis@icmc.usp.br

This paper proposes a Model Predictive Controller to safely handle longitudinal and lateral driver intents up to the limits of handling on front wheel driven vehicles. The main contributions of this work are a variation of the nonlinear bicycle model to reduce the influence of nonlinear term during the MPC optimization and coupling both longitudinal and lateral controllers using a force circle. Stability near saturating limits is calculated by model linearization and real-time tire/road friction estimation. A state estimation capable of reliably estimating the vehicle lateral speed is assumed. The control law is designed such that the rear tire and the front tire never saturate and the vehicle never exceeds maximum stable yaw rate boundaries.

The rest of this paper is organized as follows: Section II presents the vehicle models used; Section describes the proposed controllers controller; Section IV presents and discusses simulations results; Finally Section V presents concluding remarks and future work.

II. VEHICLE MODEL

This section describes the nonlinear bicycle model for a front wheel driven and the proposed force input-based nonlinear bicycle model. Both models are described directly by the influence of tire forces on angular and linear accelerations. For that purpose a tire model capable of modeling saturation limits is necessary. In this paper the Fiala tire model [6] has been chosen due to its parameters been directly related to tire characteristics and due to its relative low complexity.

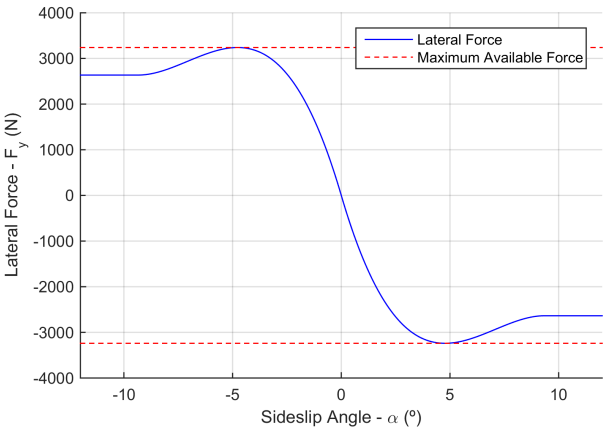

Fig. 1. Fiala tire model

A. Fiala Tire Model

There are three categories of models capable of representing the tire dynamics on saturation situations: Finite element analysis [7] [8]; Through empirical data approximation, such as the "Magic Tire Formula" [9] and the dynamical approximation of the tire by a "brush" model first proposed by Fiala [6]. Between those, the third modeling technique, shown in Figure 1, presents a good compromise between its ability to describe tires physical properties and its complexity, since it assumes that the tire is always at steady state and tire transients are faster than chassis transients.

This model is parameterized for a given tire i by its sideslip angle (α_i), cornering stiffness (C_i), static friction coefficient (μ), tire normal force (F_z) and ratio between dynamical and static friction coefficients (R_μ) as:

$$f(\alpha_i) = C_i tan(\alpha_i)$$
$$F_{yi} = \begin{cases} -f(\alpha_i) + \frac{2-R_\mu}{3\mu F_{zi}}|f(\alpha_i)|f(\alpha_i)\dots \\ -\frac{1-\frac{2}{3}R_\mu}{(3\mu F_{zi})^2}f(\alpha_i)^3, & |\alpha_i| \leq tan^{-1}\left(\frac{3\mu F_{zi}}{C_i}\right) \\ -sign(\alpha_i)\mu_s F_{zi}, & otherwise \end{cases} \quad (1)$$

where $|\alpha_i| > tan^{-1}(3\mu F_{zi}/C_i)$ is the tire full saturation region.

Given the polynomial form model, the peak lateral force and its sideslip angle can be analytically obtained:

$$q = \left(1 - \frac{2}{3}R_{mu}\right)^{-1}$$
$$F_{yi}^{peak} = \mu F_{zi}(-q + \frac{2-R_{mu}}{3}q^2 + \frac{1-\frac{2}{3}R_{mu}}{9}q^3) \quad (2)$$
$$\alpha_i^{peak} = tan^{-1}\left(\frac{q\mu F_{zi}}{C_i}\right)$$

B. Nonlinear Bicycle Model

The bicycle model is a simplification of the car dynamics where the left and right front wheels are replaced by a virtual front wheel in the center of the front axle. Analogously, the left and right rear wheels are replaced by a virtual wheel in the center of the rear axle. A representation of a vehicle on this form is shown in Figure 2.

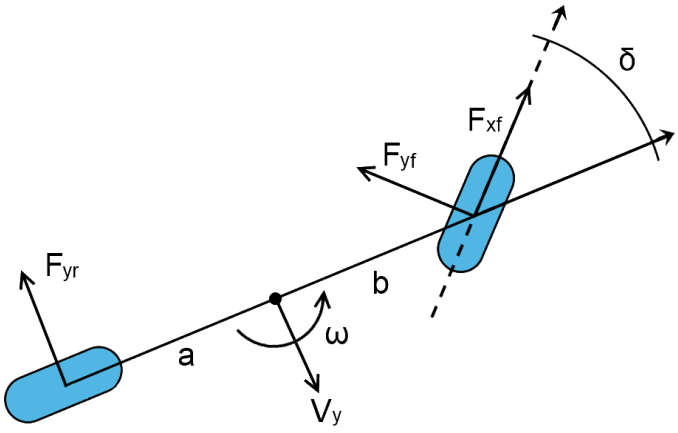

Fig. 2. Nonlinear bicycle model

Its nonlinear form is given directly by the equations of motion for a state $x(t) = [v_x(t), v_y(t), \omega(t)]^T$ and input $u(t) = [F_{xf}, \delta]^T$, where $v_x(t)$ is the longitudinal speed in the chassis frame, $v_y(t)$ is the lateral speed, $\omega(t)$ is the yaw rate, δ is the front wheel steering and F_{xf} is the front tire longitudinal force:

$$\dot{v}_x = \frac{1}{m}(F_{xf}cos(\delta) - F_{yf}sin(\delta)) + \omega v_y$$
$$\dot{v}_y = \frac{1}{m}(F_{xf}sin(\delta) + F_{yf}cos(\delta) + F_{yr}) - \omega v_x \quad (3)$$
$$\dot{\omega} = \frac{1}{I_z}(aF_{yf}cos(\delta) + aF_{xf}sin(\delta) - bF_{yr})$$

Lateral forces F_{yf} and F_{yr} are given by the Fiala tire model with sideslip angles α_f and α_r given by:

$$\alpha_f = tan^{-1}\left(\frac{v_y + a\omega}{v_x}\right) - \delta$$
$$\alpha_f = tan^{-1}\left(\frac{v_y - b\omega}{v_x}\right) \quad (4)$$

C. Force Input-based Nonlinear Bicycle Model

Beal and Gerdes [4] proposed a variation of the linear bicycle model using the front tire lateral force as a controllable input, reducing the influence of nonlinear terms during the optimization. However, such model does not allow the development of a coupled MPC controller. This paper proposes the use of Beal's concept on a nonlinear bicycle model to incorporate longitudinal speed into the model.

For that purpose the inverse Fiala tire model ($\alpha_f(F_{yf}^{desired})$) is obtained as the numerical solution to:

$$F_{yf}(\alpha_f) - F_{yf}^{desired} = 0 \quad (5)$$

and consequently the steering angle (δ) is given by:

$$\delta = tan^{-1}\left(\frac{v_y + a\omega}{v_x}\right) - \alpha_f(F_{yf}^{desired}) \quad (6)$$

For the rest of the paper $F_{yf}^{desired}$ will be simply referred to as F_{yf} for a more compact notation.

Analogously to the standard nonlinear model, this is given directly by the equations of motion from Equation 3 for a state $x(t) = [v_x(t), v_y(t), \omega(t)]^T$ and input $u(t) = [F_{xf}, F_{yf}]^T$ where the rear tire is still given by the Fiala tire model.

III. VEHICLE CONTROLLER

The controller primary objective is to ensure driver and vehicle safety, avoiding tire saturation. Secondarily, it should follow the drivers intent as close as possible and avoid uncomfortable interventions. Given these objectives, this section describes modeling linearization and discretization, driver intent modeling, safety constraints and the proposed MPC based on these characteristics.

A. Model Linearization and Discretization

In order to develop a real time model predictive controller, the optimization function must be convex and quadratic. For this reason the system model must be linearized. Given the current state $x(t)$ and current input $u(t)$ the force input-based nonlinear model is represented using a first order Taylor-approximation:

$$\dot{x}(t+\tau) = A^c\left(x(t+\tau) - x(t)\right) + B^c\left(u(t+\tau) - u(t)\right) + \dot{x}(t) \tag{7}$$

where:

$$A^c = \left.\frac{\partial \dot{x}(x,u)}{\partial x}\right|_{x=x(t)} \qquad B^c = \left.\frac{\partial \dot{x}(x,u)}{\partial u}\right|_{u=u(t)} \tag{8}$$

Subsequently, the model is discretized and represented in the form $x(k+1) = Ax(k) + Bu(k) + f$ using Euler integration with n sub-steps:

$$A = (I_{n_x} + \frac{Ts}{n}A^c)^n \tag{9}$$

$$B = \left(\sum_{i=0}^{n-1}\left(I_{n_x} + \frac{Ts}{n}A^c\right)^i\right)B^c \tag{10}$$

$$f = \left(\sum_{i=0}^{n-1}\left(I_{n_x} + \frac{Ts}{n}A^c\right)^i\right)\left(\dot{x}(t) - A^c x(t) - B^c u(t)\right) \tag{11}$$

where n is chosen high enough that A, B and f converge.

B. Representing Driver Intent

Finding a good representation of how the driver perceives the vehicle is essential to maintaining comfort and predictability of the assisted driving system. Average drivers knowledge of transients is limited, however the transients cannot be disregarded on the reference model as this would lead to harsh uncomfortable actuations.

If the nonlinear bicycle model is linearized on $x = [v_x(t), 0, 0]^T$ and $u = [0, 0]^T$, Equation 3 can be rewritten as:

$$\begin{aligned}
\dot{v}_x &= \frac{F_{xf}}{m} \\
\dot{v}_y &= -\frac{C_f + C_r}{m}v_y - \left(\frac{aC_f - bC_r}{mv_x} - v_x\right)\omega + \frac{C_f}{m}\delta \\
\dot{\omega} &= -\frac{aC_f - bC_r}{I_z}v_y - \frac{a^2C_f + b^2C_r}{I_z v_x}\omega + \frac{aC_f}{I_z}\delta
\end{aligned} \tag{12}$$

where v_y and ω are analogous to the linear bicycle model [10].

The linearized system described in Equation 12 can be discretized as previously proposed and represented in canonical form $x_d(k+1) = A_d x_d(k) + B_d u_d(k)$ with block diagonal matrices A_d and B_d as the motion of the state v_x is decoupled from the motion of states v_y and ω. The driver's input $u_d(k)$ is assumed constant and a reference consisting of $[x_d(k)\ x_d(k+1)\ \ldots\ x_d(k+N)]$ is defined as the user intent.

C. Safety Handling Boundaries

Vehicle loss-of-control situations occur when one or more tires saturate, therefore maintaining vehicle controllability is analogous to avoiding tire saturation.

On a front wheel driven vehicle as the one studied in this paper, no longitudinal forces are applied to the rear tire. Erlien et al. [11] presented a Envelope Controller proposed by Beal [4] where two constraints are used for rear wheel saturation avoidance: One limiting the rear sideslip angle (dashed red lines) and one limiting the yaw rate (blue lines), as shown in Figure 3. These constraints are adapted for the controller proposed in this paper.

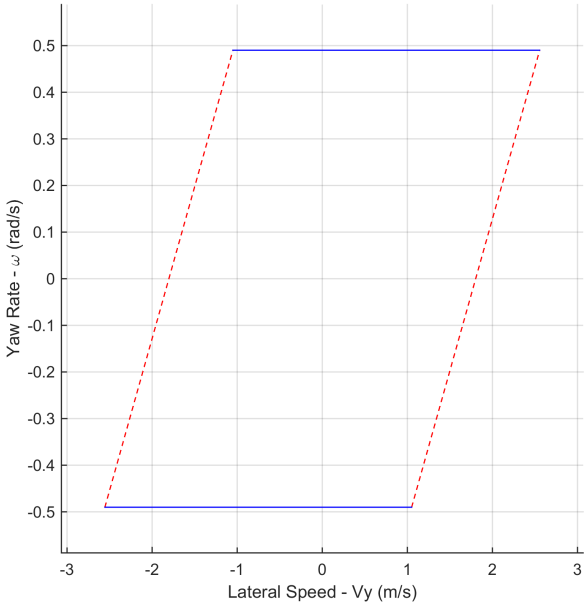

Fig. 3. Yaw rate and rear sideslip constraints

Based on the sideslip definition on Equation 4, a bound constraint can be expressed as:

$$\left|tan^{-1}\left(\frac{v_y - b\omega}{v_x}\right)\right| \leq \alpha^{max} \tag{13}$$

where, for the safe handling of a average driver $\alpha^{max} = \alpha^{peak}$ resulting:

$$\left|tan^{-1}\left(\frac{v_y - b\omega}{v_x}\right)\right| \leq tan^{-1}\left(\frac{q\mu F_{zr}}{C_r}\right) \tag{14}$$

which can be written in linear form:

$$-\frac{q\mu F_{zr}}{C_r}v_x \leq v_y - b\omega \leq \frac{q\mu F_{zr}}{C_r}v_x \tag{15}$$

The yaw rate constraint is used to ensure that the operation envelope is stable. It is defined as the maximum stable yaw rate for a given longitudinal speed, since maximum cornering occurs for F_{xf} = 0, the maximum yaw rate can be dynamically obtained as:

$$\omega^{max} = \frac{\mu}{v_x}\frac{ab + max(a,b)^2}{min(a,b)(a+b)} \tag{16}$$

and the yaw rate constraint can be expressed as:

$$-\omega^{max} \leq \omega \leq \omega^{max} \tag{17}$$

As both F_{xf} and F_{yf} are control inputs. A constraint must be applied to control inputs to avoid front wheel saturation. The saturation avoidance is given by the l^2-norm restriction:

$$F_{xf}^2 + F_{yf}^2 \leq \mu^2 F_{zf}^2 \tag{18}$$

however, using convex quadratical constraints have a significant impact on the solver performance, for this reason this constraint was tightened and approximated by eight linear constraints as shown in Figure 4 which will be compactly represented as:

$$H_f u(k) \leq G_f \tag{19}$$

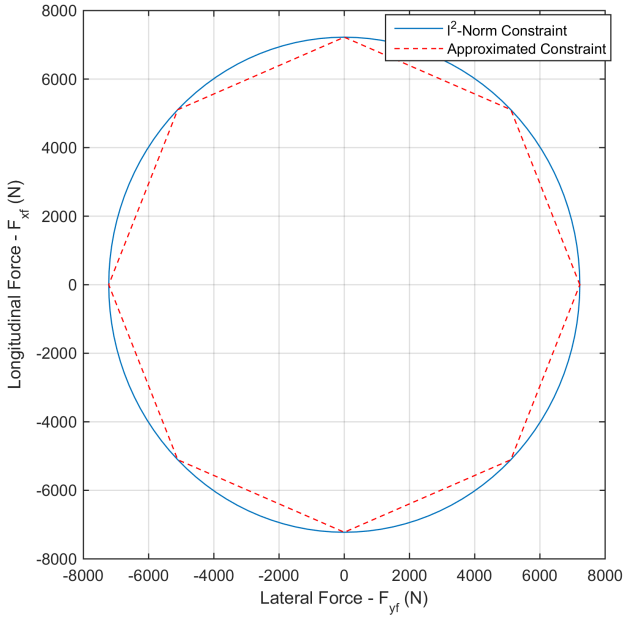

Fig. 4. Front wheel force constraints

D. Proposed Model Predictive Controller

The presented constraints are essential for fulfilling the controllers primary objective of ensuring the driver, passengers and vehicle safety. Besides ensuring safety, the controller should be non invasive to the driver during non-saturating moments. Both objectives can be expressed as a optimization objective for a MPC as:

$$\begin{aligned} min_u \quad & \textstyle\sum_{k=0}^{N}(x(k)-x_d(k))^T Q(x(k)-x_d(k)) + \dots \\ & \textstyle\sum_{k=0}^{N-1} u(k)^T R u(k) \\ s.t. \quad & x(k+1) = Ax(k) + Bu(k) + f \;\; \forall k \in [0, N-1] \\ & x_d(k+1) = A_d x_d(k) + B_d u_d(k) \;\; \forall k \in [0, N-1] \\ & -\tfrac{q\mu F_{zr}}{C_r} v_x(k) \leq v_y(k) - b\omega(k) \leq \tfrac{q\mu F_{zr}}{C_r} \;\; \forall k \in [0, N] \\ & -\omega^{max} \leq \omega(k) \leq \omega^{max} \;\; \forall k \in [0, N] \\ & H_f u(k) \leq G_f \;\; \forall k \in [0, N-1] \\ & -u_{slew}^{max} \leq u(k) - u(k-1) \leq u_{slew}^{max} \;\; \forall k \in [1, N-1] \end{aligned} \tag{20}$$

where the control inputs $u(k) = [F_{xf}(k), F_{yf}(k)]^T$ for N time steps are the output variables of the optimization. And only $u(0)$ will be applied to the vehicle as the optimization will be re-solved in the next time step. State error cost matrix Q can be expressed as:

$$Q = \begin{bmatrix} W_{v_x} & 0 & 0 \\ 0 & W_{v_y} & 0 \\ 0 & 0 & W_\omega \end{bmatrix} \tag{21}$$

where W_{v_x}, W_{v_y} and W_ω are the costs related to longitudinal speed, lateral speed and yaw rate, respectively. And control input error cost matrix R can be expressed as:

$$R = \begin{bmatrix} W_{F_{xf}} & 0 \\ 0 & W_{F_{yf}} \end{bmatrix} \tag{22}$$

where $W_{F_{xf}}$ and $W_{F_{xf}}$ are the costs related to longitudinal and lateral forces, respectively. Besides the constraints presented on Section III-C, control slew is constrained by u_{slew}^{max}, based on the maximal δF possible by the powertrain and brakes for the longitudinal force and steering for lateral force. Table I presents the parameters values used for the proposed controller.

TABLE I
CONTROLLER PARAMETERS

Parameter	Symbol	Value	Unit
Prediction horizon	N	10	–
Longitudinal speed weight	W_{v_x}	1	s^2/m^2
Lateral Speed weight	W_{v_y}	1	s^2/m^2
Yaw rate weight	W_ω	1	s^2
Longitudinal force weight	$W_{F_{xf}}$	10^{-10}	$1/N^2$
Lateral force weight	$W_{F_{yf}}$	10^{-10}	$1/N^2$
Maximum yaw rate	ω^{max}	[1]	$1/s$
Maximum input slew	u_{slew}^{max}	[1]	N
Operation frequency	-	100	Hz

FORCES [12] was used for real time solver code generation. THe resulting controller has a worst case execution time of $214\mu s$ on a Intel i7-4510U 2.GHz, it utilizes 7184 bytes of memory and has a worst case processing of 354210 floating point operations per cycle.

IV. SIMULATION RESULTS

Two simulations scenarios were evaluated: The first assumes a vehicle with fully decoupled steer-by-wire system and the second assumes a mechanical redundant steer-by-wire where wheels have a $2deg$ maximal deviation for actuation. In both scenarios a vehicle at $20m/s$ enter a slalom maneuver turning the hand wheel as a sinusoidal function at $0.25Hz$ and $10deg$ amplitude while setting a brake intent of $1000N$.

A. Fully Decoupled Steer-by-Wire

The first evaluated scenario studies the ideal case where a fully decoupled Steer-by-Wire system is featured, this serves to validate the controller capabilities. The vehicle initial

[1]Parameter dynamically evaluated during control loop

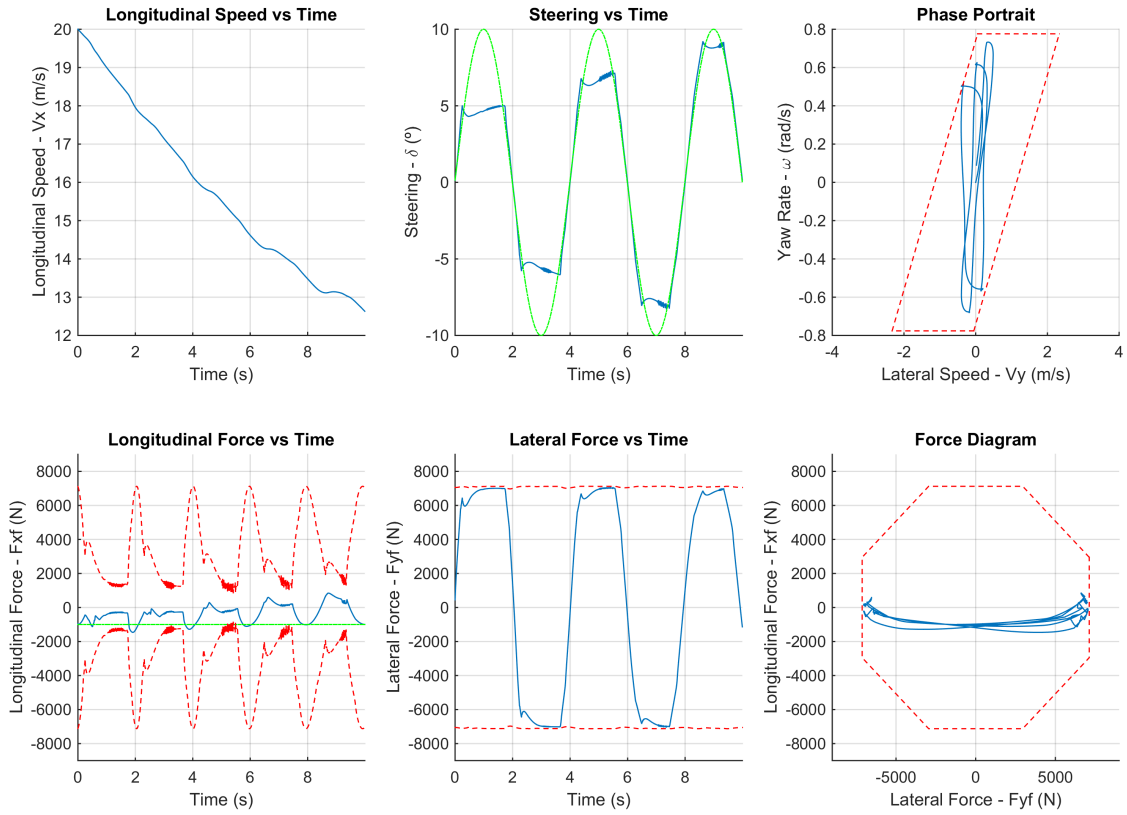

Fig. 5. Simulation results for first scenario

TABLE II
SIMULATED VEHICLE PARAMETERS

Parameter	Symbol	Value	Unit
Vehicle mass	m	1231	Kg
Inertia Moment z	I_z	2034.5	$\frac{Kg}{m^2}$
Front axle distance to CG	a	1.07	m
Back axle distance to CG	b	1.53	m
Front tire cornering stiffness	C_f	120000	$\frac{N}{rad}$
Rear tire cornering stiffness	C_r	175000	$\frac{N}{rad}$
Tire-road friction coefficient	μ	1	-

condition was $x = [20, 0, 0]^T$ and $u = [0, 0]^T$ and the drivers input steer was defined by a sinusoidal function. Results for this simulation are shown in Figure 5, from top left to bottom right are, respectively, the longitudinal speed profile, steering profile, lateral speed by yaw rate phase portrait, longitudinal front tire force, lateral front tire force and longitudinal by lateral tire force diagram. For each graphic, blue continuous line represents the simulated vehicle data, green continuous line represents the driver intention and red dashed lines represent system boundaries.

It is possible to observe that when the vehicle is far from saturation limits the steering and braking relates closely with the desired by the driver.

Since braking with front or rear tires limits the maximal lateral force, during near saturation situations the braking is inferior to the desired value by the driver since keeping the desired tracking curvature is more important than the acceleration, therefore all available tire force is used as lateral tire force.

B. *Mechanical Redundancy Constrained Steer-by-Wire*

Since a mechanical redundancy for Steer-by-Wire are currently necessary for robustness and system failure, the second evaluated scenario studies the case of a limited actuation for the controller to change wheel angles. This serves to validate the controller under harder situations where saturation might not be avoidable. As the first scenario, the vehicle initial condition was $x = [20, 0, 0]^T$ and $u = [0, 0]^T$ and the drivers input steer was defined by a sinusoidal function.

Results for this simulation are shown in Figure 6, where the graphics are organized as the first simulation results. In this simulation it is possible to observe that the longitudinal force is maintained at the intended by the driver since the lateral force saturates independently of the longitudinal force. It is also possible to observe in that once the front tire saturates the vehicle returns to the central region of the phase portrait. This undesired result might be mitigated using differential braking.

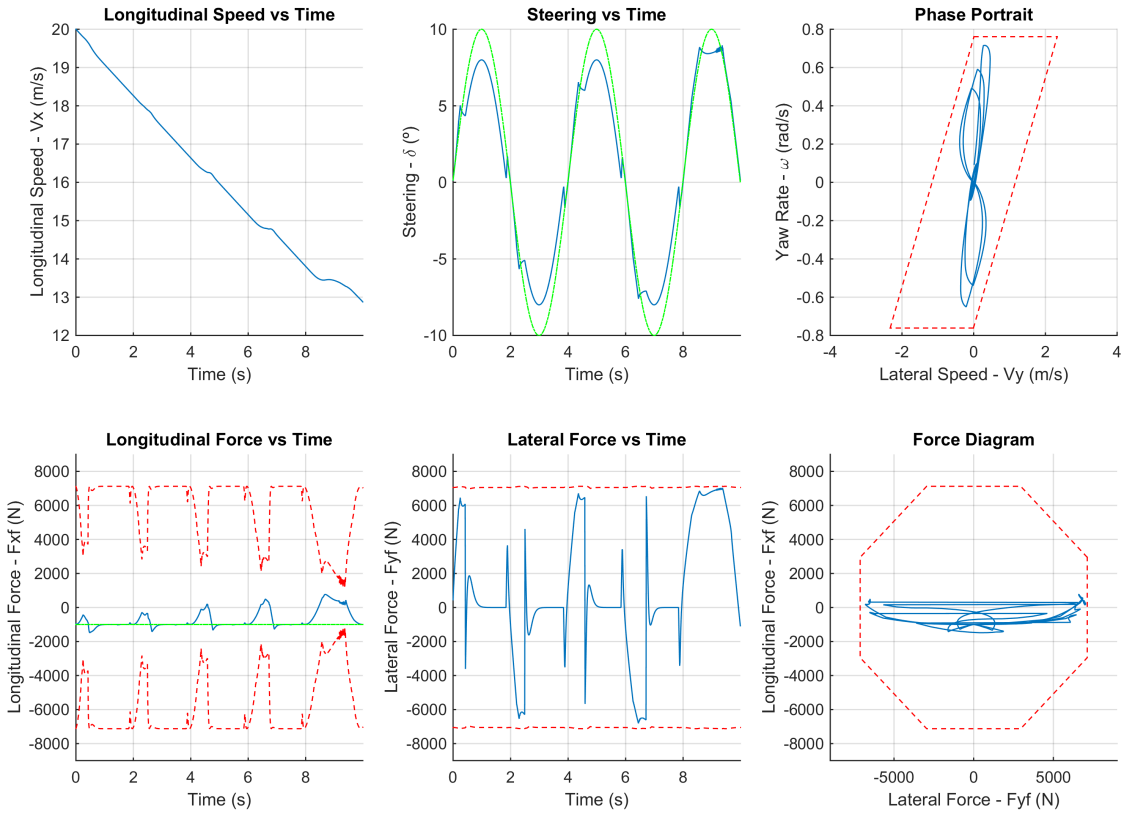

Fig. 6. Simulation results for first scenario

V. CONCLUSIONS

In this paper a coupled longitudinal and lateral Steer-by-Wire driver assistance system using Model Predictive Control was proposed. Front and rear tire saturation limits where defined as operation boundaries in order to avoid loss-of-control situations. Also, a variation of the nonlinear bicycle model based on previous work from Beal and Gerdes was proposed to reduce the influence of nonlinear terms on the coupled modeling.

Since in a mechanical redundant Steer-by-Wire system there is no possibility of avoiding wheel saturation, joint differential braking and active front steering will be required for safely tracking the drivers intent. For this reason future work will focus on extending the proposed method to differential braking and internalizing estimation uncertainty.

REFERENCES

[1] K. Koibuchi, M. Yamamoto, Y. Fukada, and S. Inagaki, "Vehicle stability control in limit cornering by active brake," *SAE Paper*, 1996.

[2] Y.-H. Hsu, S. M. Laws, and J. C. Gerdes, "Estimation of tire slip angle and friction limits using steering torque," *Control Systems Technology, IEEE Transactions on*, vol. 18, no. 4, pp. 896–907, 2010.

[3] H. Hamann, J. K. Hedrick, S. Rhode, and F. Gauterin, "Tire force estimation for a passenger vehicle with the unscented kalman filter," in *Intelligent Vehicles Symposium Proceedings, 2014 IEEE*. IEEE, 2014, pp. 814–819.

[4] C. Beal and J. Gerdes, "Model predictive control for vehicle stabilization at the limits of handling," *Control Systems Technology, IEEE Transactions on*, vol. 21, no. 4, pp. 1258–1269, July 2013.

[5] A. Carvalho, Y. Gao, A. Gray, H. Tseng, and F. Borrelli, "Predictive control of an autonomous ground vehicle using an iterative linearization approach," in *Intelligent Transportation Systems - (ITSC), 2013 16th International IEEE Conference on*, Oct 2013, pp. 2335–2340.

[6] E. Fiala, "Kraftfahrzeugtechnik," in *Dubbel*. Springer, 1987, pp. 941–966.

[7] P. Helnwein, C. H. Liu, G. Meschke, and H. A. Mang, "A new 3-d finite element model for cord-reinforced rubber composites—application to analysis of automobile tires," *Finite elements in analysis and design*, vol. 14, no. 1, pp. 1–16, 1993.

[8] M. Koishi, K. Kabe, and M. Shiratori, "Tire cornering simulation using an explicit finite element analysis code," *Tire Science and Technology*, vol. 26, no. 2, pp. 109–119, 1998.

[9] H. B. Pacejka and E. Bakker, "The magic formula tyre model," *Vehicle system dynamics*, vol. 21, no. S1, pp. 1–18, 1992.

[10] C. Massera Filho and D. F. Wolf, "Dynamic inversion-based control for front wheel drive autonomous ground vehicles near the limits of handling," in *Intelligent Transportation Systems (ITSC), 2014 IEEE 17th International Conference on*. IEEE, 2014, pp. 2138–2143.

[11] S. M. Erlien, J. Funke, and J. C. Gerdes, "Incorporating non-linear tire dynamics into a convex approach to shared steering control," in *American Control Conference (ACC), 2014*. IEEE, 2014, pp. 3468–3473.

[12] A. Domahidi, A. Zgraggen, M. Zeilinger, M. Morari, and C. Jones, "Efficient interior point methods for multistage problems arising in receding horizon control," in *IEEE Conference on Decision and Control (CDC)*, Maui, HI, USA, Dec. 2012, pp. 668 – 674.